Influence of the cylindrical anisotropy of wood on the structural behaviour of holes in glued-laminated timber beams

Tomas Hermsen[1]

ABSTRACT: Introducing holes in glulam beams disrupts the stress flow, causing redistribution of shear and bending stresses around the hole. This redistribution leads to tensile stresses perp. to the grain and increased shear stresses in the vicinity of a hole. The failure mechanism is well manifested and involves crack propagation along the grain of unreinforced and reinforced holes at the location where the tensile stresses reach their maximum. Experimental tests showed cracks consistently initiated near the mid-width of the cross-section due to the cylindrical anisotropy of wood. This study investigated the cylindrical anisotropy of wood on the structural behaviour of holes in glulam beams. A comparative analysis between the orthotropic and cylindrical anisotropic models demonstrates an inhomogeneous stress distribution with pronounced stress peaks for the cylindrical anisotropic model. The study investigated the influence of three reinforcement scenarios: 1 rod, 2 rods and plywood panels. Rods placed at an angle of 45° achieve the most significant reductions for these pronounced stress peaks, particularly in the scenario with a single rod.

KEYWORDS: Glulam, Holes, Cylindrical anisotropy of wood, Reinforcements, FEM, Tensile stresses perp. to the grain

1 INTRODUCTION

Introducing holes in beams made of glued laminated timber (glulam) is a common application in practice. They create a path for plumbing, electrical and other service-relevant infrastructure if these cannot be placed under or around the beam for architectural, aesthetic, or other reasons. The introduction of the hole disrupts the stress flow in the beam and leads to the redistribution of shear, and bending stresses around the hole. This redistribution generates tensile stresses perp. to the grain and increased shear stresses in the vicinity of the hole, which were not present before introducing the hole. Especially the tensile stresses perp. to the grain are of concern since the strength of timber in this direction is relatively low. Therefore, the stress concentrations can reduce the load-bearing capacity of the beam significantly.

The failure mechanism of unreinforced and reinforced holes is well known. It involves crack propagation in the direction along the grain in two diagonally opposed regions starting at the location where the tensile stresses perp. to the grain reaches its maximum. The first crack usually appears in the upper right quadrant (towards mid-span), followed by the lower left quadrant (towards support). The cracks propagate until a sudden brittle failure occurs, usually at the left bottom quadrant of the hole. It was identified that the tensile stresses perp. to grain is the primary reason for crack initiation [1].

The design of holes according to design standards revolves around calculating a fictive tensile force composed of two additive components: a shear and moment component, each representing the respective part of the stresses that must be redistributed around the hole [2]. The force must be resisted by either the volume-dependent fictive tensile resistance of the glulam or by reinforcements. Reinforcements can increase the load-bearing capacity and prevent or even halt the propagation of cracks. The concept of reinforcements is to increase the tensile strength perp. to the grain locally in the regions where cracks are expected to occur. There are two types of reinforcements: internal and external reinforcements. Generally, internal reinforcements are preferred since they are concealed in the glulam and are easier to install at a relatively low cost.

Literature [3][4][5] reported that cracks always initiated near the mid-width of the cross-section, regardless of whether the hole was reinforced or not. This behaviour was attributed to the cylindrical anisotropy of wood [3], which leads to an inhomogeneous stress and strain distribution along the cross-sectional width with a pronounced stress peak near the mid-width. The inhomogeneous stress and strain distribution along the width at the face of the hole were also verified experimentally [6]. These observations underscore the importance of considering the cylindrical anisotropy of wood to accurately approximate the stress distribution in the vicinity of an unreinforced and reinforced hole [7].

For most structural applications, timber is assumed to be orthotropic and even a two-dimensional transverse isotropic material. Thus only making a distinction between the parallel and perp. to the grain direction. This simplification is justified because the stiffness in the longitudinal direction is far greater than in the radial and tangential directions, the two perp. to the grain directions. The stiffness in the perp. direction is taken as the smeared average of the radial and tangential stiffness [8], and plane stress is assumed in the width direction. However, these simplifications lead to an inadequate approximation for applications where the stresses perp. to the grain govern the design, such as holes in glulam beams.

[1] Tomas Hermsen, Technische Universiteit Eindhoven, Netherlands, t.m.hermsen@student.tue.nl

The cylindrical anisotropic model results in a more accurate approximation but is more complex than the usual orthotropic or transverse isotropic approximation used for most structural applications. To implement the cylindrical anisotropic model, the cylindrical orientations of the individual laminations to the pith of the tree stem they were sawn from are essential parameters. Furthermore, the difference between the radial and tangential stiffness and the low rolling shear stiffness contribute to the inhomogeneous stress distribution [8]. Noteworthy, the cylindrical anisotropy of wood does not affect the stresses parallel to the grain [8].

So far, only Tapia [9] investigated the influence of the cylindrical anisotropic model to glulam beams with holes numerically. However, the cylindrical anisotropic model was omitted for the remainder of his thesis due to the dependency of the pith orientations in a glulam cross-section. All other literature regarding holes in glulam is based on orthotropic or transverse isotropic behaviour. Therefore, this paper aims to study the influence of the cylindrical anisotropy of wood on the structural behaviour of a glulam beam with a circular hole through a numerical study. The effect of the cylindrical anisotropy on the stress distribution in the vicinity of an unreinforced and reinforced hole will be discussed. Additionally, the damaged state is also examined.

2 STRUCTURAL BEHAVIOUR

2.1 Tensile stresses perp. to the grain

Glulam beams with holes are generally subjected to a combined shear and moment action and, on some rare occasions, to pure moment action. Introducing a hole disturbs the stress flow of the shear and bending stresses and causes tensile stresses perp. to the grain at distinct locations along the periphery of the hole. The magnitude and location of the hole depend on the loading situation.

Figure 1 depicts the distribution of the stresses perp. to the grain for a circular hole subjected to a combined shear and moment action. The pattern consists of two sets of diagonally opposed regions, resulting in an anti-symmetric pattern. The tensile stresses for this load configuration arise in the bottom and right top quadrant (when placed left from a point load). Compressive stresses are present in the remaining two quadrants. The angle φ indicates where the largest tensile stress perp. to the grain along the periphery arises in the case of circular holes and, consequently, where cracks are likely to initiate. The angle φ is within the range of 40° (+180°) ≤ φ ≤ 60° (+180°) for a circular hole subjected to a combined shear and moment action [10]. The angle of the upper right region is close to 45°, while the lower left region has a slightly bigger angle. Additionally, the figure indicates the crack planes at which the cracks initiate and propagate. Literature reported that cracks initiated at the top right quadrant first.

2.2 Shear stress concentrations

Besides the tensile stresses perp. to the grain, the shear stresses are also important to consider. The shear stresses

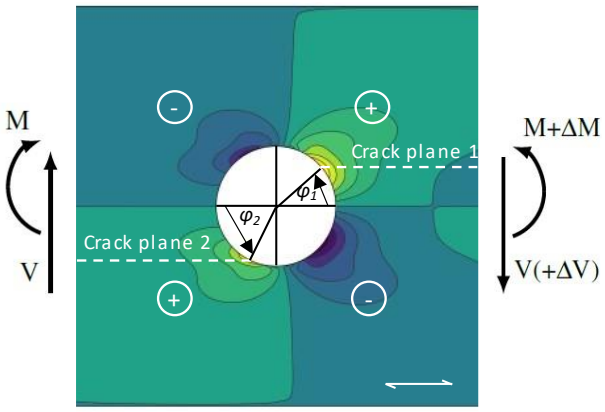

Figure 1: *Stresses perp. to the grain in the vicinity of a circular hole with a hole height of 0.3h and a M/V ratio of 5h.*

differ considerably from the distribution obtained according to beam theory at the hole's periphery. The deviation becomes more significant closer to the hole, with pronounced stress peaks at the periphery. Figure 2 illustrates the shear stresses in the vicinity of a circular hole. The pattern is different from the tensile stresses perp. to the grain. The shear stresses plotted over a vertical path at the edge of the hole are also shown.

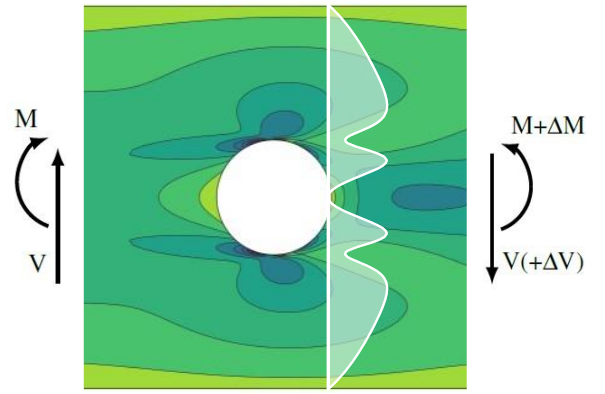

Figure 2: *Shear in the vicinity of a circular hole with a hole height of 0.3h and a M/V ratio of 5h.*

2.3 Design of holes acc. design standards

The design of a beam with a hole revolves around calculating a fictive tensile force $F_{t,90}$. This fictive tensile force comprises two additive components: a shear component $F_{t,90,V}$ and a moment component $F_{t,90,M}$. The fictive tensile strength of the glulam must resist this fictive tensile force. This fictive tensile resistance depends on a volume-dependent tensile strength. If this resistance is insufficient, additional measurements must be applied in the form of reinforcements.

The current version of Eurocode 5 [11] contains no rules or regulations regarding holes in glulam beams. However, the national annex of Germany [12] does dedicate a section to the design of holes in glulam beams. The approach is based on the work of Kolb & Epple [13], but it was shown that the moment component needs

amendments [2]. The future generation of Eurocode 5 [14] will include a section for the design of holes in glulam beams based on the research of Danzer et al. [5].

2.4 Reinforcements

Reinforcements must be designed for the full fictive tensile force. Thus, neglecting the glulam's contribution equals a fully cracked cross-section. However, literature [15][16] showed that the internal and external reinforcements share this force with the glulam in the undamaged state.

It was shown that vertically placed rods are ineffective in reducing the tensile stresses perp. to the grain and shear stresses [17]. However, when the rods are placed under an angle of 45°, significant increases in the load-bearing capacity and reductions of the tensile stresses perp. to the grain and shear stresses are obtained [18][16][5]. Furthermore, it was shown that holes reinforced with plywood increased the load at which the first crack initiates significantly and even achieved the total characteristic shear capacity of a beam without a hole [19].

Generally, externally reinforced holes are preferred since larger holes are allowed by the design standards for externally reinforced holes. This preference is based on the consensus that panel-like reinforcements better reduce shear stresses. However, research has shown that inclined rods also effectively reduce shear stresses [16].

3 CYLINDRICAL ANISOTROPY OF WOOD

Trees grow in two directions: longitudinally and radially. Longitudinal growth happens vertically along the length of the tree stem, while radial growth occurs over the course of a year, forming concentric rings called annual rings. Radial growth is driven by cell division in the cambium during the growing season from spring to autumn in the Northern Hemisphere. The annual rings, classified as earlywood and latewood, are visible in a cross-section of the tree stem. Earlywood, formed in spring, has thin-walled cells and serves to transport water and nutrition. Latewood, formed in summer, prioritises strength and has thicker-walled cells with a darker colour.

The mechanical properties of the wood perp. to the stem are affected by the yearly addition of new wood in the radial direction. The longitudinal direction and the perp. plane have significantly different mechanical properties. To simplify the tree stem, it is often approximated as a conical shape with decreasing diameter along the height. This conical can be further simplified to a cylindrical shape. This simplified cylindrical model is easier to implement in Finite Elements programs. The cylindrical anisotropic model defines three principal material directions: longitudinal, radial, and tangential. The periodic variations in mechanical properties caused by earlywood and latewood are typically ignored at the macro scale, treating the wood as a quasi-homogeneous continuum [20]. This material behaviour does not consider growth irregularities like knots and resin pockets.

The laminations are obtained by sawing rectangular cross-sections parallel to the pith of the stem. The sawing disrupts the cylindrical orientation within the tree trunk. The orientation to the pith defines the local coordinate system of an individual lamination. It strongly depends on the employed sawing pattern and the specific location within the tree trunk. The pith marks the centre of the local cylindrical coordinate system in the laminations. Two additional parameters, *d* and *e*, define the local coordinate system. The parameter *d* represents the distance from the pith to the bottom face of the lamination, while *e* denotes the eccentricity of the pith from the mid-width of the lamination. Figure 3 depicts the just-described concept.

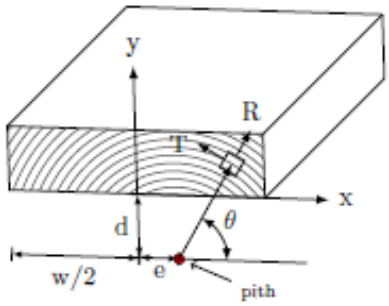

***Figure 3**: Definition of the local cylindrical material coordinate system of an individual lamination [9].*

The manufacturing process of a glulam cross-section involves gluing multiple laminations together. As each lamination is obtained from a distinct position within the tree trunk, it possesses a unique cylindrical coordinate system. Thus, to accurately model a glulam cross-section, it is necessary to specify the orientation of each lamination relative to the pith from the stem it was sawn. Specifying every individual orientation is tedious since every lamination will have a unique orientation. Therefore, the study adopted similar lay-up patterns as Aicher & Dill-Langer [20], as depicted in Figure 4.

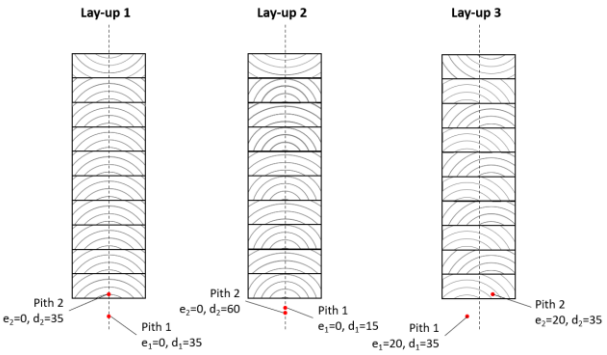

***Figure 4:** Employed lay-up patterns for this study.*

4 Methodology

4.1 Studied configuration

The study focused on a circular hole placed along the beam neutral axis of the beam, as shown in Figure 5. The circular hole has a height of 120 mm (0.3*h*) and is positioned at a distance ℓ_v of 2*h* away from the support and point load. The beam has a height *h* of 400 mm, a total length of 1.925 mm and a width *w* of 120 mm. The parameters above are enough to describe the geometry of the orthotropic model. However, the cylindrical anisotropic models require additional parameters related to the individual laminations. The thickness of the laminations is 40 mm, resulting in 10 laminations for a beam with a height of 400 mm. The employed lay-up patterns are depicted in Figure 4. A total of 4 cases are considered: one orthotropic reference case and three cylindrical anisotropic cases.

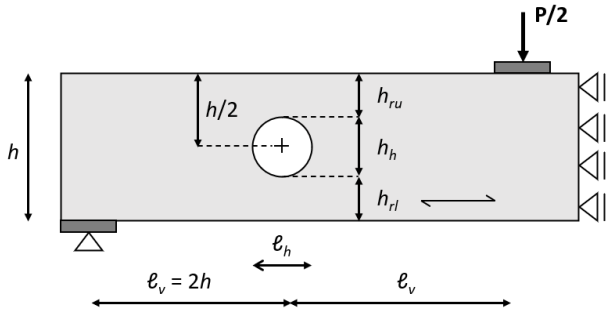

***Figure 5**: Studied hole configuration.*

Three different reinforcement scenarios were considered. The first scenario considered a single rod with a diameter d_r of 14 mm installed at the mid-width of the cross-section. The second scenario considered two rods with a diameter d_r of 10 mm installed next to each other along the cross-sectional width. The rods were placed at an angle of inclination β of 45° for both scenarios. It was found that a rod placed at an angle of 45° was the most effective for reducing the tensile stresses perp. to the grain and shear stresses [16]. The rods were placed a distance of $a_{3,c}$ from the location of the maximum tensile stress. The last scenario considered a plywood panel made of birch glued to both sides of the glulam beam with a length and height of 280 mm and a thickness, t_r of 24 mm. Figure 6 represents the three reinforcement scenarios.

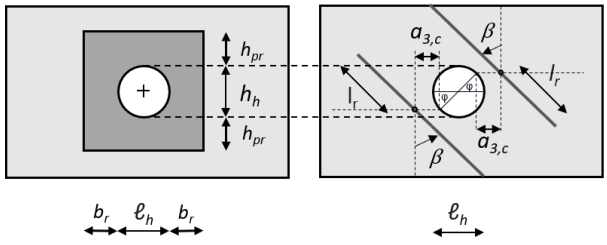

***Figure 6**: The three studied reinforcement scenarios.*

The constitutive properties of the glulam for the orthotropic model correspond to strength class GL24h according to EN 14080 [22]. The constitutive properties of the cylindrical anisotropic models are based on the stiffness ratios proposed by Aicher & Dill-Langer [20]. The constitutive properties are summarised in Table 1 along with the properties used for the birch plywood panels.

4.2 Finite element models

The software Abaqus v2019 [21] with its standard solver was used. Different models were created to analyse the stress distribution in the vicinity of a hole. Python scripting, employing the Object-Oriented Programming (OOP) approach, is used to parameterise the models, accelerate the modelling process, and facilitate post-processing of results.

4.2.1 Unreinforced

The glulam is modelled as a 3D solid deformable part using linear continuum elements with reduced integration (C3D8R and C3D6 for some cells in the cylindrical anisotropic models). Symmetry conditions were applied in the *YZ*-plane at the mid-span of the beam and in the *XY*-plane at the mid-width of the cross-section, except for lay-up 3. Both orthotropic and cylindrical anisotropic models were discretised using elements with a width of 4 mm. The size of the elements was 2 mm along the periphery of the hole and increased to 5 mm in a region extending 250 mm on both sides of the hole. Beyond this region, the element size gradually increased further away to a size of 20 mm. In the case of the cylindrical anisotropic model, the height of the laminations going through the hole was discretised by 20 elements, 10 elements in the laminations directly above and below the hole and 5 elements for the remaining laminations. This results in a total amount of elements of approximately 430.000 for the orthotropic model and 520.000 for the cylindrical anisotropic model. The meshing of the orthotropic and cylindrical anisotropic models is depicted in Figure 7.

Rigid elements of type R3D4 were used to model the support and load plate. The dimension of the plates is 250 mm x 40 mm x 120 mm (l x h x w). A reference point was placed at the centre of the load plate to introduce the point load. The point load for the quarter beam was 2.500 N and 5.000 N for the complete cross-section in case of lay-up 3. Another reference point was positioned near the centre of the support plate to apply the boundary condition. The support and load plate were connected with tie constraints to the glulam beam.

4.2.2 Internal reinforced

The internally reinforced models were created based on the repository provided by Tapia [12]. The modelling was done "manually" due to the complex nature of the internally reinforced cylindrical anisotropic models. Continuum linear elements with reduced integration (C3D8R) were used for the rods. The rods were discretised by elements with a width of 3 mm. Tie constraints were used to connect the respective surface pairs in contact with the rods and glulam beam.

***Table 1**: Constitutive properties used for the Finite Element Models.*

Strength class	Ref	E_x / E_L	E_y / E_R	E_z / E_T	G_{xy} / G_{LR}	G_{xz} / G_{LT}	G_{yz} / G_{RT}	v_{xy} / v_{LR}	v_{xz} / v_{LT}	v_{yz} / v_{RT}
		(N/mm²)			(N/mm²)			(-)		
GL24h orth.	[22]	11.500	300	300	650	650	65	0,02	0,02	0,3
GL24h cy. an.	[20]	11.500	1.065	715	715	715	45	0,02	0,02	0,3
Plywood	[15]	9.100	8.400	370	620	620	50	0,04	0,4	0,4

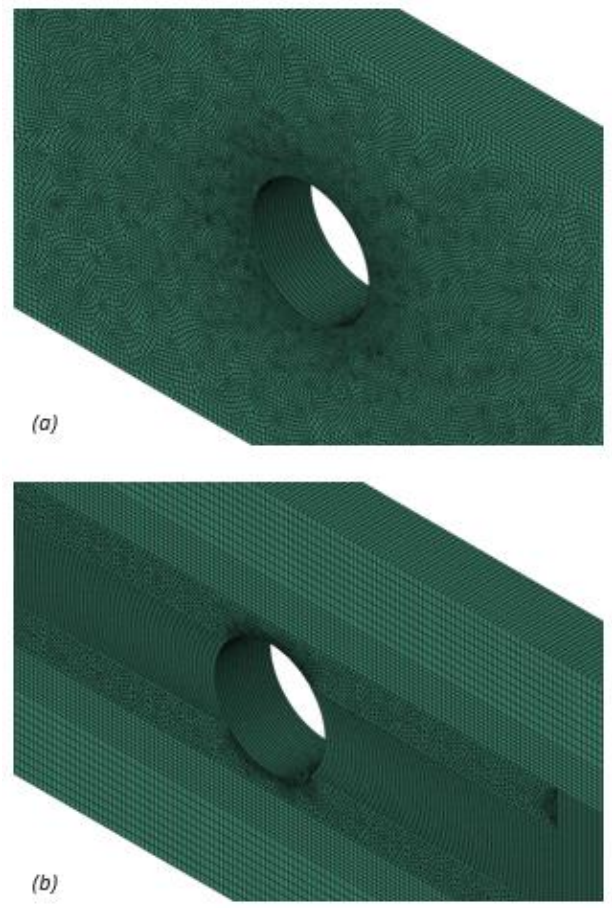

***Figure 7:** Discretisation of the FEM models in the vicinity of the hole. (a) Orthotropic model; (b) Cylindrical anisotropic model.*

The elements at the periphery of the hole had a size of 2 mm, which increased to a size of 3 mm to the rods. The meshing of the glulam was done similarly to the unreinforced models. The Youngs modulus of the steel E is 210.000 N/mm², and the Poisson ratio v is 0.3.

4.2.3 Damaged state

The Extended Finite Element Method (XFEM) was employed to model a stationary crack parallel to the grain direction of the beam to evaluate the impact of the different crack stages on the stress redistribution in the glulam at the region of the highest tensile stresses. At the location of the crack, an unmeshed surface was placed, cutting all the enriched elements it intersected. Because only a stationary crack was considered, neither crack extension nor fracture mechanics were considered.

Three distinct crack stages are defined between crack initiation and the extension of the crack to the outer edges of the glulam. Some simplifications had to be made due to the complex geometry of the cracks observed in the experimental tests. Because the cracks are modelled as a flat surface, no curvature analogous to the growth rings is considered. The damaged state is only considered for the cylindrical anisotropic case employing lay-up pattern 1.

4.3 Post-processing

The Python scripts included a function to obtain the necessary results from the models. This function calculated the fictive tensile force and located the maximum tensile stress perp. to the grain along the periphery of the hole.

The function first located the maximum tensile stress perp. to the grain along the periphery of the hole. The coordinates of the point are saved and used to create a horizontal path at each z-position where element nodes are present. This horizontal path lasts $2h_h$ and extends away from the hole. Along this path, the stresses perp. to the grain are integrated until they reach a value of zero. The result is then multiplied by the width of an element. Finally, the values obtained along each path are added to get the total fictive tensile force. The results of this calculation are saved to a text file, together with the maximum tensile stress perp. to the grain.

5 RESULTS

5.1 Unreinforced situation

Figure 8 depicts the tensile stresses along the width of the cross-section at the location where the tensile stresses perp. to the grain reaches its maximum. An inhomogeneous distribution of the tensile stresses perp. to the grain is observed with pronounced stress peaks near the mid-width of the cross-section for the three cylindrical anisotropic cases. In contrast, the stresses in the orthotropic case remain constant along the width. Lay-up 2, with a periodically varying pith distance d, had the most pronounced stress peak with a maximum of 1.9 times greater than the orthotropic case. Lay-up 1 had a slightly lower peak (1.8). The stress peak of lay-up 3, with a periodically varying eccentricity e, has a less pronounced stress peak of 1.5 times the orthotropic case. Furthermore,

lay-up 3 has an offset like the eccentricity of the pith from the mid-width. An eccentrically placed pith positively influences the magnitude of the tensile stress peak. Notably, the stresses at the outer edges of the glulam are considerably lower for the three cylindrical anisotropic cases compared to the orthotropic case.

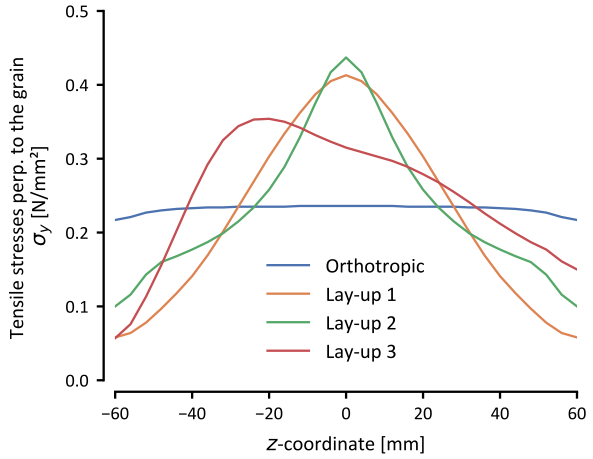

Figure 8: *Tensile stresses perp. to the grain along the width at the location where the tensile stresses reach their maximum along the periphery of the hole.*

rods is on the lower side of the range. The reduction ranges from 20% to 26% for the plywood panel. The orthotropic case shows a 28% and 15% reduction for the rods and panel, respectively. The magnitude of the reduction strongly depends on the eccentricity e of the pith for the scenarios with rods. In contrast, the influence of the eccentricity e was less pronounced for the plywood panels. Furthermore, the comparison between the orthotropic and cylindrical anisotropic cases reveals that the reductions are situated near the stress peak for the cylindrical anisotropic cases. In contrast, for the orthotropic cases, the reduction is somewhat present along the full cross-sectional width.

The tensile stresses perp. to the grain for the reinforced state along crack plane 1 are depicted in Figure 11. The red area indicates the stresses perp. to the grain in the reinforced state, while the yellow area represents the stresses in the unreinforced state. The figure reveals that the scenario where a single rod is present obtains the most significant reduction of the tensile stresses perp. to the grain, followed by the scenario with two rods. The plywood panels are the least effective. The tensile stresses perp. to the grain are almost entirely taken by the rods in the region preceding the rod, while the tensile stresses remain present over a longer distance away from the hole for the panels. Like the cylindrical anisotropic models, the single rod is also the most effective for the orthotropic case, although the reduction pattern differs.

(a) depicts the tensile stresses perp. to the grain along crack plane 1 for the orthotropic case and lay-up 1. For the orthotropic case, the stresses are evenly distributed along the width and gradually decrease over a distance away from the hole. On the contrary, lay-up 1 shows an inhomogeneous stress distribution along the width of crack plane 1. The tensile stresses decrease more significantly over a distance away from the hole. The figure shows that the tensile stresses are concentrated near the mid-width at the face of the hole and are remarkably low at the outer edges. This concentration of stresses is a reasonable explanation for the observed behaviour in the experimental tests, where cracks consistently initiated near the mid-width. Therefore, the need to reduce this pronounced stress peak cannot be questioned. Although not shown, similar patterns are observed for lay-ups 2 and 3. Based on these observations, one might suggest that a rod directly placed at the stress peak is the most effective type of reinforcement.

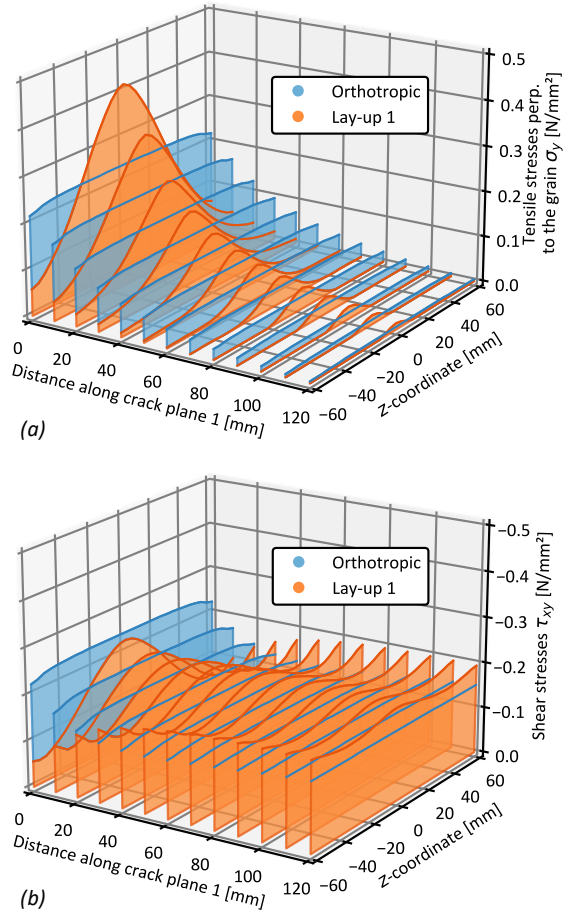

Figure 9: *(a) Tensile stresses perp. to the grain; (b) Shear stresses along crack plane 1.*

The shear stresses along crack plane 1 are depicted in Figure 9 (b). Like the tensile stresses perp. to the grain, an inhomogeneous distribution of the shear stresses is observed at the face of the hole for lay-up 1. However, this inhomogeneous stress distribution becomes more homogeneous at a distance away from the hole. Noteworthy is that the magnitude of the shear stress peaks for the cylindrical anisotropic cases is similar to the orthotropic case. At the same time, they are significantly lower at the outer edges. The shear stresses along a horizontal path at mid-width ($z = 0$) show that the shear stresses for the cylindrical anisotropic cases remain somewhat constant. In contrast, the shear stresses increase if one looks at a horizontal path at the outer edges ($z = \pm 60$). Although not shown, this is also observed for lay-

ups 2 and 3. The opposite can be said for the orthotropic case, where the shear stresses are more significant at the face of the hole and slightly decrease over a small distance from the hole. Based on these observations, it can be stated that the cylindrical anisotropy of wood is more favourable for the shear stresses than the commonly applied orthotropic representation.

The fictive tensile force $F_{t,90}$ is an important concept in the design of holes since it determines whether the glulam has enough resistance against this force. The study revealed that the cylindrical anisotropy of wood had a positive effect on the magnitude of the fictive tensile force, resulting in forces that are approximately 15% (lay-ups 1 and 2) to 30% (lay-up 3) lower compared to the orthotropic case. Thus, assuming orthotropic behaviour results in a conservative approximation of this fictive tensile force.

5.2 Reinforced situation

Figure 11 presents the tensile stresses along a similar path as Figure 12, but then for the reinforced situation. The solid lines represent the unreinforced situation, while the dashed line represents the reinforced situation. It can be observed from the figure that the reinforcement scenario with a single rod is the most effective in reducing the stress peak $\sigma_{y,max}$ at the face of the hole for all four cases, followed by the scenario with two rods. The scenario where plywood panels are glued to both sides of the glulam is the least effective. The reduction of the tensile stress peak $\sigma_{y,max}$ is 19% to 48% depending on the number of rods and the considered lay-ups, where the scenario with two rods is on the lower side of the range. The reduction ranges from 20% to 26% for the plywood panel. The orthotropic case shows a 28% and 15% reduction for the rods and panel, respectively. The magnitude of the reduction strongly depends on the eccentricity e of the pith for the scenarios with rods. In contrast, the influence of the eccentricity e was less pronounced for the plywood panels. Furthermore, the comparison between the orthotropic and cylindrical anisotropic cases reveals that the reductions are situated near the stress peak for the cylindrical anisotropic cases. In contrast, for the orthotropic cases, the reduction is somewhat present along the full cross-sectional width.

The tensile stresses perp. to the grain for the reinforced state along crack plane 1 are depicted in Figure 11. The red area indicates the stresses perp. to the grain in the reinforced state, while the yellow area represents the stresses in the unreinforced state. The figure reveals that the scenario where a single rod is present obtains the most significant reduction of the tensile stresses perp. to the grain, followed by the scenario with two rods. The plywood panels are the least effective. The tensile stresses perp. to the grain are almost entirely taken by the rods in the region preceding the rod, while the tensile stresses remain present over a longer distance away from the hole for the panels. Like the cylindrical anisotropic models, the single rod is also the most effective for the orthotropic case, although the reduction pattern differs.

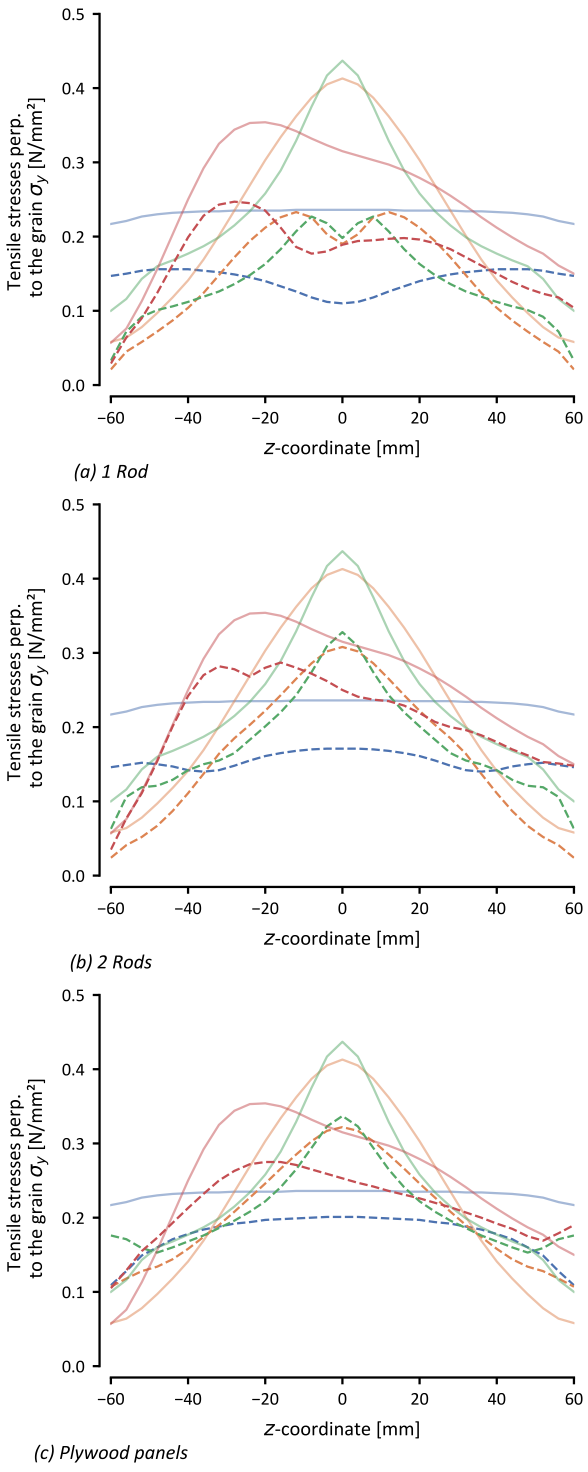

Figure 10: *Reduction of the tensile stresses perp. to the grain along the width at the location where the tensile stresses reach their maximum along the periphery of the hole for the three different reinforcement scenarios.*

The shear stresses for the reinforced state along crack plane 1 are shown in Figure 12. The figure reveals that the orthotropic case slightly overestimates the reduction of the shear stresses compared to the three cylindrical anisotropic cases. Like the tensile stresses perp. to the grain, the shear stresses are the most significantly reduced for the scenario with a single rod, followed by the scenario with two rods. Again, the plywood panels are the least

effective. For all three reinforcement scenarios, the reductions become less at a more considerable distance away from the hole. The most striking thing is that external reinforcements are often preferred due to their ability to reduce shear stresses. Nonetheless, these observations contradict this statement.

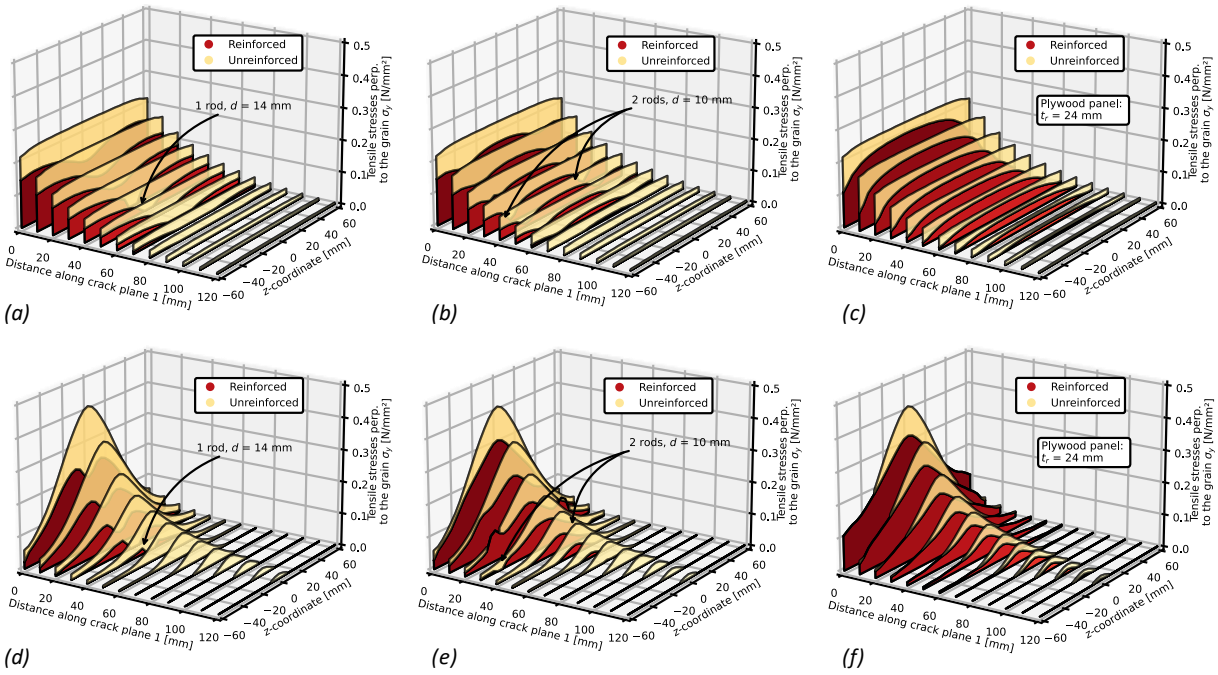

***Figure 11**: Tensile stresses perp. to the grain along crack plane 1 for the reinforced situation. (a-c) Orthotropic model; (d-f) Cylindrical anisotropic model, lay-up 1.*

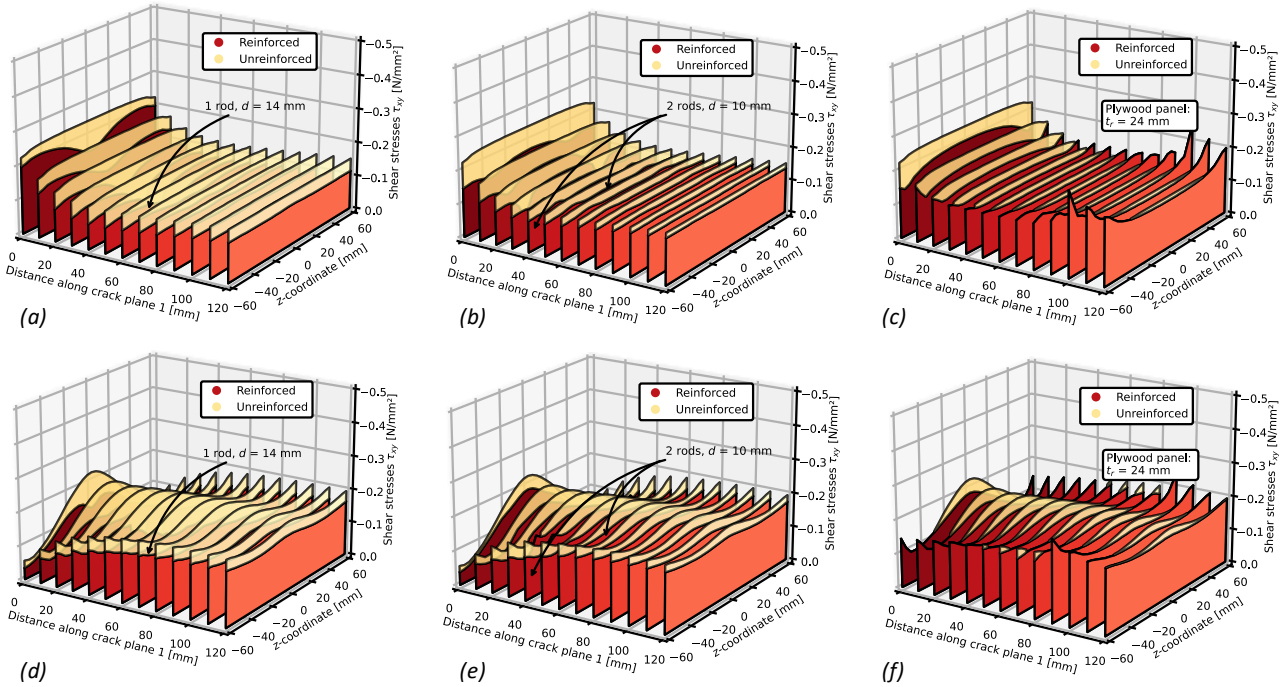

***Figure 12:** Shear stresses along crack plane 1 for the reinforced situation. (a-c) Orthotropic model; (d-f) Cylindrical anisotropic model, lay-up 1.*

The fictive tensile force is reduced the most effectively by the single rod, as one might already have suggested based on Figure 11. Furthermore, the reduction of the fictive tensile force is more significant than the reduction of the stress peak. The reduction of the fictive tensile force is 35% to 69% for the rods and 19% to 26% for the plywood panels. Significantly lower compared to the rods. This difference can be explained by the fact that the rods achieve a more significant reduction of the tensile stresses perp. to the grain. The reductions for the orthotropic case are 55% and 34% for the rods and panels, respectively, which means that the orthotropic case overestimates the reduction of the fictive tensile force for the plywood panels and represents an average of the rods compared to the cylindrical anisotropic cases.

5.3 Damaged state

Figure 13 depicts the tensile stresses perp. to the grain and the shear stresses along crack plane 1 for crack stage 3, a crack has developed along the entire width of the cross-section in the unreinforced state. The evaluation of a propagating crack showed that the cracks strongly influence the tensile stresses perp. to the grain. The peaks follow the crack tip, but they become less pronounced as the crack propagates since they are transferred by a greater surface around the crack tip. Contrarily, the distribution of the shear stresses appears unaffected by the presence of stationary cracks.

The influence of reinforcements in the damaged state was also examined. The study revealed that the presence of rods mitigates the tensile stresses perp. to the grain within the remaining glulam area. The rods progressively take more of the fictive tensile force as the crack propagates. It can even be argued that the rods can halt the crack propagation once it has reached the rods and the shear stresses remain under the shear strength. The plywood panels were not so effective in mitigating the tensile stresses perp. to the grain. Furthermore, it appears that panels can only slow down the crack propagation. Neither reinforcement scenario reduced the shear stresses significantly, indicating that the primary action for crack propagation switches to the shear stresses at a certain point.

6 CONCLUSION

The presented study revealed that the cylindrical anisotropy of wood cannot be neglected when a hole is present in a glulam beam. The cylindrical anisotropy leads to an inhomogeneous stress distribution with pronounced tensile stress peaks near the mid-width of the cross-section, thereby deviating significantly from the orthotropic case. The peaks had a magnitude of almost twice the maximum tensile stress of the orthotropic case. On the contrary, the cylindrical anisotropy positively affects the shear stresses and fictive tensile force $F_{t,90}$.

Furthermore, the cylindrical anisotropy of wood should be considered to examine the influence of reinforcements on the structural behaviour of a hole. Different reduction patterns are observed for the three cylindrical anisotropic cases compared to the orthotropic case. The study showed that rods at an angle of 45° achieved the most significant reduction of the tensile stresses perp. to the grain, shear stresses and the fictive tensile force, particularly in the scenario with a single rod. The rods may even halt the crack propagation once the crack has reached the rod.

Contrary to what is generally believed, the external reinforcements are ineffective in reducing the tensile stresses perp. to the grain and shear stresses in the vicinity of the hole. The plywood panels obtained the lowest reductions of the three reinforcement scenarios.

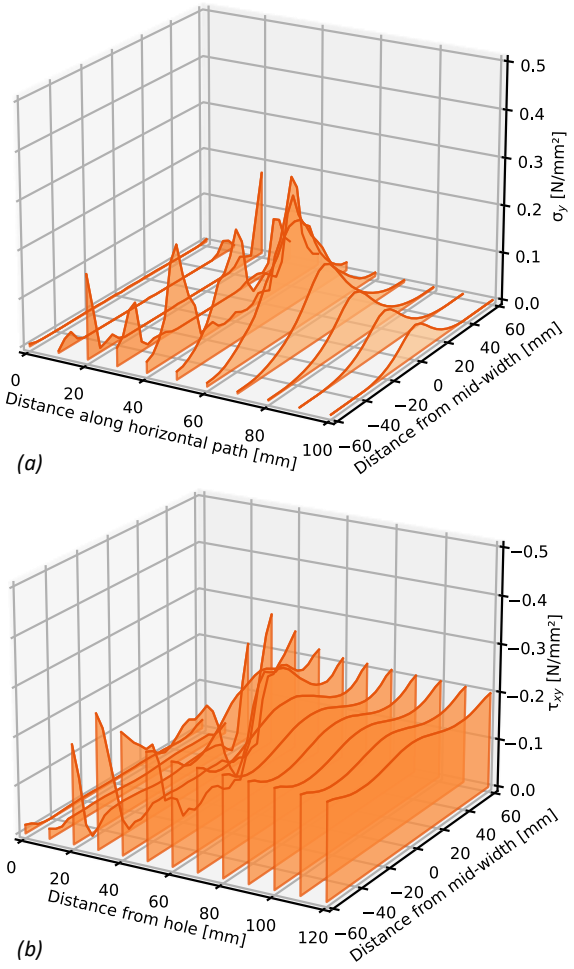

Figure 13: *(a) Tensile stresses perp. to the grain and (b) shear stresses along crack plane 1 at crack stage 3 for the unreinforced situation.*

REFERENCES

[1] Höfflin, L. Runde Durchbrüchen in Brettschichtholzträgern – Experimentelle und theoretische Untersuchungen. PhD thesis. Universität Stuttgart. 2005.

[2] Tapia, C, Aicher, S. EVALUATION OF DESIGN CONCEPTS FOR HOLES IN GLULAM BEAMS—COMPARISON WITH TEST RESULTS. Otto-Graf-Journal. 2019;18:329-44.

[3] Aicher S, Höfflin L. Tragfähigkeit und Bemessung von Brettschichtholzträgern mit runden Durchbrüchen: sicherheitsrelevante Modifikationen

der Bemessungsverfahren nach Eurocode 5 und DIN 1052. Forschungsschlussbericht DIBt-Vorhaben ZP 52-5-13.161-1092/04. Materialprüfungsanstalt Universität Stuttgart; 2006 December.

[4] Danielsson H. Strength of glulam beams with holes - Tests of quadratic holes and literature test result compilation. International Council for Research and Innovation in Building and Construction. 2008 August.

[5] Danzer M, Dietsch P, Winter S. Einfluss exzentrisch positionierter runder Einzeldurchbrücheche und Gruppen von Durchbrüchen auf die Tragfähigkeit von Brettschichtholzträgern. Munich: TUM, Lehrstuhl für Holzbau und Baukonstruktion; 2017.

[6] Aicher S, Höfflin L. Verifizierung versagensrelevanter Dehnungsverteilungen im Bereich runder Durchbrüche in Brettschichtholzträgern. Bautechnik. 2003 August; 80(8): p. 523-533.

[7] Aicher S, Höfflin L. Fracture behaviour and design of glulam beams with round holes. In Proceedings of the 10th World Conference on Timber Engineering; 2008. p. 132-140.

[8] S. Aicher and G. Dill-Langer, "Influence of cylindrical anisotropy of wood and loading conditions on off-axis stiffness and stresses of a board in tension perpendicular to the grain," Otto Graf Journal, vol. 7, 1996.

[9] Tapia C. Internal and external reinforcements for holes in glued laminated beams. Santiago: Universidad de Chili, Departamento de Ingeniería Civil; 2015.

[10] Aicher S, Höfflin L. Runde Durchbrüche in Biegeträgern aus Brettschichtholz-Teil 1: Berechnung. Bautechnik. 2001 Oct;78(10):706-15.

[11] CEN, Eurocode 5: Design of timber structures - Part 1-1: General rules and rules for buildings, in EN 1995-1-1:2004. 2004, Comité Européen de Normalisation.

[12] DIN, Nationaler Anhang - National festgelegte Parameter - Eurocode 5: Bemessung und Konstruktion von Holzbauten - Teil 1-1: Allgemeines - Allgemeine Regeln und Regeln für den hochbau, in Din EN 1995-1-1:2004/NA:2013. 2013, Deutsche Institut für Normung e.V.

[13] Kolb H, Epple A. Verstärkung von durchbrochenen Brettschichtbindern. Research Report 14-34810. Stuttgart: FMPA; 1985.

[14] CEN, Eurocode 5: Design of timber structures - Part 1-1: General rules and rules for buildings, in prEN 1995-1-1:20XX. 2021, Comité Européen de Normalisation.

[15] Aicher S. Glulam beams with internally and externally reinforced holes–Test, detailing and design. In Proceedings of the 44th CIB-W18 Meeting; 2011.

[16] Tapia C, Aicher S. Holes in glulam - Orientation and design of internal reinforcements. CDROM Proceedings of the World Conference on Timber Engineering (WCTE 2016). 2016;: p. 978.

[17] Aicher S. Glulam beams with holes reinforced by steel bars. Intl. Council for Research and Innovation in Building and Construction, Working Commission 18-Timber Structures. 2009.

[18] Blaß HJ, Bejtka I. Querzugverstärkungen in gefährdeten Bereichen mit selbstbohrenden Holzschrauben. Fraunhofer IRB Verlag. ; 2003.

[19] Aicher S, Tapia C. Glulam with laterally reinforced rectangular holes. In World Conference on Timber Engineering; 2012 July; Auckland.

[20] S. Aicher and G. Dill-Langer, "Effect of lamination anisotropy and lay-up in glued-laminated timbers," Journal of Structural Engineering, vol. 131, no. 7, pp. 1095-1103, July 2005.

[21] Abaqus v2019, Dassault Systèmes Simulia Corp. Johnston, RI, USA:; 2019.

[22] NEN-EN 14080. Timber structures - Glued laminated timber and glued solid timber - Requirements. ; 2013.